ELSEVIER

Journal of Crystal Growth 206 (1999) 322–330

JOURNAL OF CRYSTAL GROWTH

www.elsevier.nl/locate/jcrysgro

Texture formation and element partitioning in trapiche ruby

Ichiro Sunagawa[a,*], Heinz-Jürgen Bernhardt[b], Karl Schmetzer[c]

[a]*Yamanashi Institute of Gemmology and Jewellery Arts, Tokoji-machi 1955, Kofu 400-0808, Japan*
[b]*Institut für Mineralogie, Ruhr-Universität, D-44780 Bochum, Germany*
[c]*Marbacher Str. 22b, D-85238 Petershausen, Germany*

Received 1 June 1999; accepted 21 June 1999
Communicated by R. Kern

Abstract

Based on textural and compositional investigations on ruby single crystals showing textures with six arms and six growth sectors (trapiche ruby), it has been analysed how the unique texture was formed, and the element partitioning was governed by the growth mechanism. The arms were formed earlier by dendritic growth on rough interfaces, and the growth sectors by lateral growth on smooth interfaces. The arm portions consist of plural mineral phases but show a low and almost uniform Cr content in corundum throughout the extension of the arm and its branches, whereas the growth sectors are single ruby phase, but show Cr zoning parallel to the growth surfaces. Element partitioning in the earlier dendritic gowh is governed by thermodynamic parameters, whereas that of the latter layer-by-layer growth by kinetics.

Keywords: Trapiche ruby; Texture; Dendritic growth; Element partitioning; Rough and smooth interfaces

1. Introduction

Ruby single crystals showing textures with six arms and six growth sectors have recently been found in South-East Asia, most probably originating from the Mong Hsu mining area, Myanmar. Their mineralogical and gemmological properties and the textures were reported by Schmetzer et al. [1,2], and compositional mapping was performed by Schmetzer et al. [3]. They are named "trapiche ruby", after the name of "trapiche emerald" from Chivor and Muzo, Colombia which show a similar texture. "Trapiche" is a Spanish word for the sugar cane crushing gear [4].

Although detailed descriptions on the texture and composition of trapiche ruby are given in Refs. [1–3], discussions were not made on how such a unique texture was formed and why mineralogical and compositional differences appeared between the arms and growth sectors. We therefore intend to discuss these problems in the light of crystal growth mechanisms based on published data [1–3], and newly obtained chemical analyses.

The origin of textures seen in trapiche emerald from Colombia was discussed by Nassau and Jackson [4]. In this paper, they used terms "core", "arms" and "two-phase region". The "core" denoted the central clear tapered prismatic portion of

* Corresponding author. Kashiwa-cho 3-54-2, Tachikawa, Tokyo 190-0004, Japan. Tel.: + 81-42-536-2564; fax: + 81-42-535-3637.
E-mail address: sunagawa@inv.co.jp, poki@inv.co.jp (I. Sunagawa)

0022-0248/99/$ - see front matter
PII: S0022-0248(99)00331-0

better emerald quality, the "arm" the trapezohedral or trapezoidal prism portions of poorer emerald quality, and "two-phase region" dendritic portions consisting of emerald-albite two phases which separate core and arms, and between the neighbouring arms (Fig. 1a). In Refs. [1–3], "core" is used as in Ref. [4], but "ruby sector" is used to denote trapezohedral or trapezoidal ruby sectors which correspond to "arm" portions in trapiche emerald [4], and "arm" to the dendritic portions corresponding to the "two-phase regions" in trapiche emerald in Ref. [4] (Fig. 1b). The terminology is very confusing. We shall follow the terminology adopted in Refs. [1–3] in this paper. The terms "core", "growth sector" and "arm" in this paper, respectively, correspond to "core", "arm", "two-phase region" in Ref. [4] used for trapiche emerald, and to "core", "ruby sector" and "arm" used for trapiche ruby in Refs. [1–3] (compare Figs. 1a and b).

Ref. [4] was probably the earliest paper in which the absolute time required for a mineral formation was evaluated (though the evaluation was only for the time required for the transition from eutectic to single phase growth). In this respect, trapiche ruby provides us with another unique opportunity to understand mineral formation from the view point of crystal growth science.

In this paper, we will at first critically summarise the essential points on the texture and composition of trapiche ruby reported in Refs. [1–3], followed by new chemical data and discussions on the mechanism of texture formation and element partitioning.

2. Texture and chemistry

Trapiche ruby crystals show hexagonal prismatic to barrel-shaped habits, bounded by basal $\{0\,0\,0\,1\}$ and tapered and curved high indexed hexagonal dipyramidal faces, sometimes associated with small rhombohedral $\{1\,0\,\bar{1}\,1\}$ faces [1]. Although

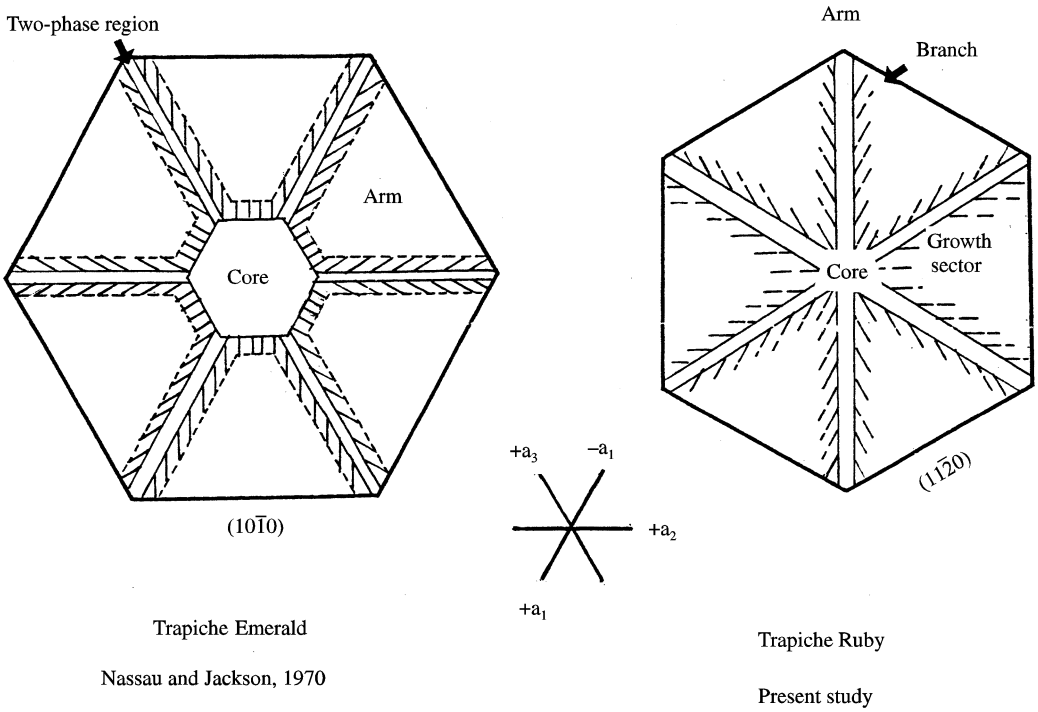

Fig. 1. Schematic illustration of textures in trapiche emerald (a) [4] and trapiche ruby (b) [1–3], together with terminology used in respective papers.

in Refs. [1,5], very high index $\{14\,14\,\overline{28}\,3\}$ was given for side faces of barrel-shaped crystals; these faces are too highly indexed to be taken as smooth faces on which layer growth takes place. Although they develop as large habit-controlling faces, they should be tapered faces consisting of alternating microsteps between $\{0\,0\,0\,1\}$ or $\{1\,1\,\bar{2}\,0\}$. They probably appeared due to selective adsorption of impurities along steps of growth layers on either $\{0\,0\,0\,1\}$ or $\{1\,1\,\bar{2}\,0\}$ faces [6]. We shall therefore call these faces, for simplicity, tapered second-order prism $\{1\,1\,\bar{2}\,0\}$ faces instead of hexagonal dipyramidal faces.

Trapiche rubies show textures consisting of six transparent-to-translucent red colour ruby growth sectors of triangular or trapezohedral form and six yellow- or white-appearing arms running from a central point or from six corners of a central hexagonal core to the six corners of the hexagonal section (six edges of hexagonal prism). The hexagonal cores are, when present, usually opaque yellow or black, having a texture similar to that of the arms, but rarely transparent red central cores are also encountered. In sections cut parallel to the *c*-axis, transparent ruby cores with tapered outline were occasionally observed, ending with opaque yellow or black portions on both ends. The boundaries of the hexagonal core and the six growth sectors are rugged and splintery. The arms extend from the edges of the core, nearly parallel to the basal plane.

On polished sections parallel or perpendicular to (0 0 0 1) faces, one notices tube-like inclusions originating from the arms and running perpendicular to the tapered prism surfaces. In Ref. [1], they were called tube-like inclusions, but in reality they are side branches of the six arms. They show colour, transparency and mineral compositions similar to those of arms and translucent to opaque yellow or black cores. On the surface of the as-grown $\{0\,0\,0\,1\}$ faces, they appear as striation-like branches, originating from the arms. The rugged and splintery appearance of the core-growth sector boundaries is due to the presence of these branches. In sections parallel to the *c*-axis, the branches appear nearly parallel to the $\{0\,0\,0\,1\}$ surface, although a slight inclination (ca. 5°) is seen, i.e. they are perpendicular to the tapered prisms. Together with solid tube-like inclusions, fluid (liquid or two-phase (liquid–gas)) inclusions are also present.

Prismatic- or barrel-shaped trapiche ruby crystals often show erroded edges, and even re-entrant angles, on hexagonal prism. This is due to weathering, preferentially attacking the edges of hexagonal prisms, i.e. outcrops of the arms. The surface of growth sectors are less weathered, but rough showing no growth step patterns. In Fig. 1, the textures of trapiche ruby are schematically illustrated (Fig. 1b), in comparison to those of trapiche emerald [4] (Fig. 1a). In Fig. 2, a photograph of a sample with polished (0 0 0 1) surface is presented.

By means of X-ray microfluorescence (XRMF) analysis and electron microprobe analysis (EPMA), element mapping (Mg, Al, Si, Ca, Ti, V, Cr, Fe) was performed on six slices of trapiche rubies cut perpendicular to the *c*-axis [3]. A beam diameter of 70 μm was adopted in the XRMF analysis. An example of the element mapping is shown in Fig. 3, and the general tendency observed is summarised in Table 1. These results clearly indicate the differences in chemistry and mineralogy between arms, cores and growth sectors.

We may summarise the important features of trapiche ruby as follows, by critically analysing the descriptions in Refs. [1–3].

(1) The skeleton of a barrel-shaped trapiche ruby is constructed by (a) tapered core, (b) dendritic arms extending along the bisecting directions of *a*-axes (parallel to $[1\,1\,\bar{2}\,0]$ axes), (c) branches from the arms running along the *a*-axes (parallel to $[1\,0\,\bar{1}\,0]$ axes) and perpendicular to tapered $\{1\,1\,\bar{2}\,0\}$ faces, and (d) growth sectors, see Fig. 1.

(2) The spaces between the arms are occupied by transparent ruby growth sectors, where Cr zoning parallel to tapered $\{1\,1\,\bar{2}\,0\}$ faces is seen. The core portions usually consist of densely developed dendritic arms and branches. At the centre of core portions, single ruby phase is sometimes present, which shows similar chemistry as that of growth sectors.

(3) The growth sectors and the rarely encountered transparent ruby core are chemically homogeneous, except for Cr zoning, consisting of single ruby phase. The widely encountered opaque cores, arms and branches

are chemically heterogeneous, and consist of intermingled minute grains of corundum, calcite, dolomite and in some samples unidentified K–Al–Fe–Ti silicate minerals, as well as fluid and two-phase inclusions.

Fig. 2. An example of trapiche ruby showing textures, with polished (0 0 0 1) surface. Sample B, about 3.3 mm across.

(4) Cr zoning is seen parallel to the hexagonal outline of the crystal in the growth sectors. No Cr zoning is detected either from the root to the tip of one arm, or between neighbouring arms, or between arms, branches and opaque cores. The Cr contents in the transparent ruby core are similar to those in the growth sectors, and are higher than those in the arms and branches.

(5) A distinct Fe zoning is seen between intensely weathered outer parts of yellow arms and less weathered inner parts of yellowish white arms. Such Fe zoning is not observed in the growth sectors.

To confirm the difference and variation of Cr contents between growth sectors and arms and branches, and within a growth sector, quantitative analyses of Al_2O_3, TiO_2, Cr_2O_3, FeO and V_2O_3 were made by EPMA, with much smaller beam diameter and narrower point distances. Sample No. B, with pointed centre, Fig. 2, was used for these analyses. Five scan directions and the corresponding plots of analytical data are shown in Fig. 4.

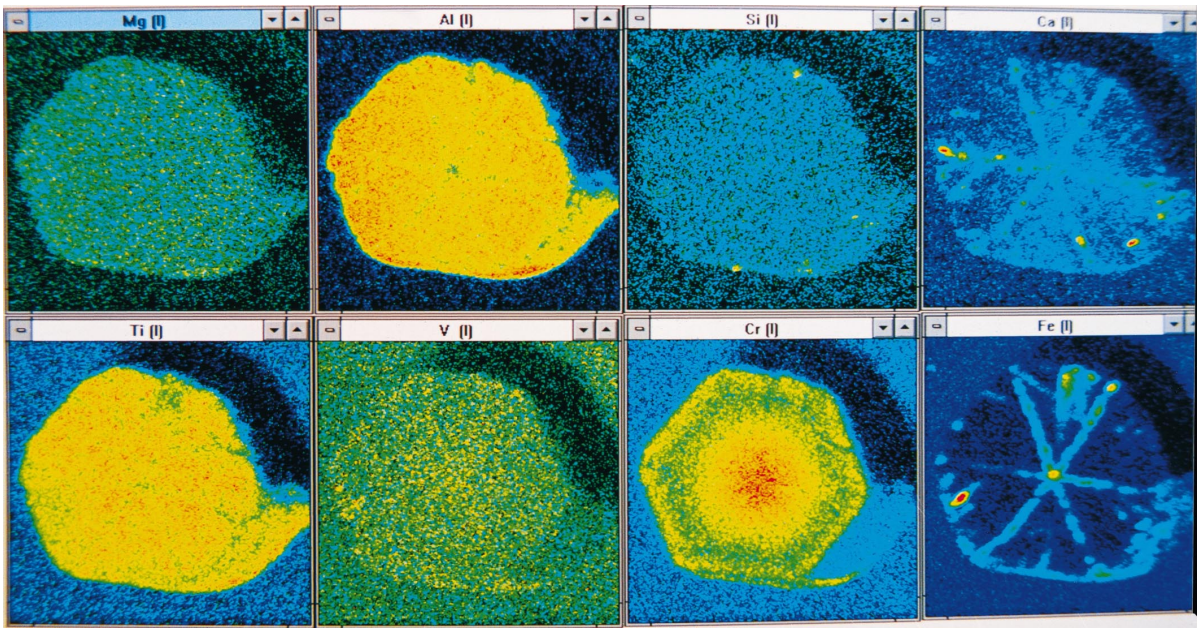

Fig. 3. An example of element mapping of (0 0 0 1) section of trapiche rubies by XRMF. Sample B. Beam diameter 70 μm.

Table 1
Summary of results of element mapping of trapiche ruby by XRMF (abbreviated from a table Ref. [3]). (S) Growth sectors, (C) core, A arms. (#) Strongly weathered sample; (−) smaller concentration than in the growth sectors; (− −) much smaller concentration than in the growth sectors; (+) higher concentration than in the growth sectors; (+ +) much higher concentration than in the growth sectors; (+ + +) very much higher concentration than in the growth sector; (z) zoning from centre to rim; (*) not observable due to an overlap of VK_α with TiK_β

Samples		Mg	Al	Si	Ca	Ti	V	Cr	Fe
(A) Sharp yellowish white arms interesecting at one point	S							z	
	A		− −	+	+ +			−	+
(B) Sharp yellow arms intersecting at one point	S							z	
	A		−		+ +				+ +
(C) Sharp yellow arms, black core	S								
	C		−	+	+ + +	+	*	−	+ +
	A		−	+	+ +	+	*		+ + +
(D) Yellow arms widening towards the edge, black core	S								
	C		− −	+	+ +	+	*		+ + +
	A		− −	+	+ +	+	*		+ + +
(E) Sharp yellowish white (inner part) to yellow (outer part) arms, black core #	S							z	
	C		−		+ +			−	+
	A		−		+ +				+ or + + (z)
(F) Yellow arms without distinct continuous boundaries, small red core	S							z	
	C							+	
	A		−		+				+

Only the plots of Al_2O_3 and Cr_2O_3 contents are given in this figure, except for scan A, where TiO_2 plots are also shown. The analyses along scans A and B were done at point distances of about 20 μm, and a beam diameter about 1 μm, for an extension of 1.5–1.6 mm (100 points each). The analyses along scans 1, 2 and 3 were done at point distances of 3 μm for 300 μm extension (100 points each), and a beam diameter of 1 μm, with long counting times, 100 s for each element on peak maximum and background.

The analytical data show the following, which re-confirm the general tendencies summarised above in a more quantitative way (Fig. 4).

(1) Cr contents of corundum points, showing Al_2O_3 contents higher than 98% in the core with dendritic texture, arms and branches, are definitely much lower than those in the growth sectors. They are almost uniform and range between 0.20 and 0.30%, much lower than those of growth sectors, if only reliable data (corundum having Al_2O_3 content higher than 98%) are used. As compared to uniform and low Cr contents in these portions, the Cr contents in growth sectors are much higher than dendritic portions and vary from 0.60 to 1.70%.

(2) Judging from the Cr contents in the data showing Al_2O_3 contents below 10% (corresponding to carbonate phase) in dendritic portions, Cr contents in the original carbonate rock are estimated to be ca. 0.10% or lower.

(3) Distinct chemical zoning in Cr contents is seen from centre to rim within one growth sector, see scans A and B in Fig. 4. Distinct and sharp increase in Cr content is noted at the onset of growth sector formation, 1.70% as compared to 0.20–0.40% in corundum in the core (although these data are of less pure corundum, having Al_2O_3 contents of 85–97%) and below 0.1% in carbonate (showing Al_2O_3 contents below 10%) in the core. Cr contents increase more than eight times at the onset of growth sectors. The Cr content decreases nearly

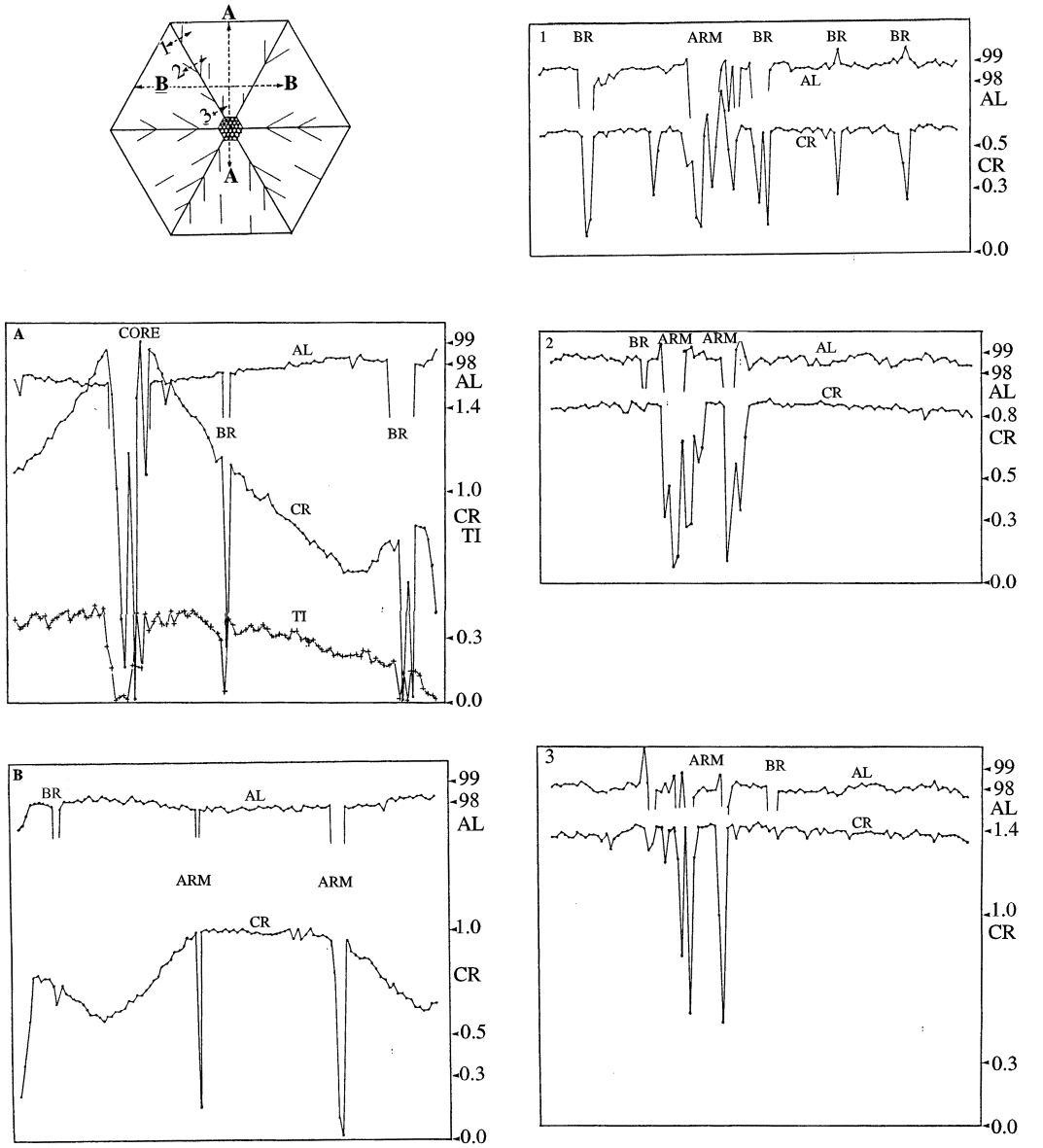

Fig. 4. Position of scans A, B, and 1–3 (a), and corresponding plots of microprobe analyses of Al_2O_3 (AL), Cr_2O_3 (CR) and TiO_2 (TI) (b) and Al_2O_3, Cr_2O_3 (c–f). In (b–f), core indicates opaque core portion, arm and br indicate, respectively, arms and branches. Sample B. Note that Al_2O_3 contents below 98 wt% indicate that the measuring point was completely or partly on calcite or dolomite or in a cavity (originally a fluid inclusion).

monotonically from this point as growth proceeds, down to 0.60%, and increases again to 0.80%, followed by a second decrease to 0.40% at the final stage, the outer rim (see also Fig. 3).

(4) Ti shows similar chemical zoning although in a much weaker manner than Cr. Starting at 0.40% at the boundary of the core to the growth sector, TiO_2 gradually decreases to

0.30% as growth proceeds and at the final stage to below 0.10%. The general tendency is concordant with that of Cr up to the point where Cr content increases again, but reverses after this point, showing monotonic decrease throughout growth process.

3. Discussion

3.1. Texture formation

Among the features summarised above, there will be no necessity to give additional explanation to conclude that Fe zoning in the arms is due to Fe infiltration during the weathering process. Since the arms have multi-phases and are full of defects and fluid filled cavities as compared to more homogeneous and perfect growth sectors, Fe infiltration proceeded faster in the arms than in the growth sectors. We shall not, therefore, discuss the origin of Fe zoning any more.

Based on the texture from mineral and chemical compositions, it is safe to conclude that the yellow or black and opaque cores, arms and branches are of the same origin. They were formed earlier than and under different kinetic parameters from the formation of growth sectors.

From the dendritic morphology and mineral compositions, yellow or black and opaque cores, arms and branches were formed by dendritic growth of corundum under eutectic growth conditions of corundum, carbonate and unidentified K–Al–Fe–Ti–silicate phases. We may take this stage as representing eutectic multiphase stage, following the terminology in Ref. [4]. Co-existing calcite and dolomite in these parts show distinct dendritic pattern on element mapping, and are considered to have been co-precipitated together with corundum and silicate phases. The presence of fluid and two phase inclusions suggests fluid state at the time of dendritic formation. We, therefore, assume that corundum, silicate and carbonate were co-precipitated from fluid phase, when dendritic growth took place.

The dendritic growth might have taken place either from the very beginning of corundum formation, or it might have been preceded by ordinary single ruby phase growth. In the latter case, a clear ruby tapered core was formed at first, on which dendritic growth took place. Such a situation is less commonly encountered than the former case in trapiche ruby, but is more common in trapiche emerald [4].

For dendritic and eutectic multi-phase growth to take place, we have to assume higher driving force condition and rougher interface than those for ordinary smooth interface growth to take place. During this stage, the skeleton of a trapiche ruby crystal, and its present size was constructed. Following this stage, and as lowering the driving force, interfaces transformed from rough to smooth on $\{0\,0\,0\,1\}$ and $\{1\,1\,\bar{2}\,0\}$. Ordinary layer-by-layer growth mechanism started to operate principally on smooth interfaces of $\{0\,0\,0\,1\}$ and $\{1\,1\,\bar{2}\,0\}$. Ruby growth sectors were formed during this stage in the interstices of already formed skeletons. The two stages are not necessarily discontinuous, with a time lag, but might have taken place almost concurrently. The dendrite tips protruded and were confronted with ambient phase of higher driving force, which resulted in rapid dendritic growth, whereas their roots became depleted where layer-by-layer growth on smooth interfaces took place.

Sunagawa [6] discussed the relations among polyhedral, hopper, dendritic, spherulitic and fractal morphology, and the expected internal morphology of crystals, when crystals grow under nonconfined condition. The discussion was based on the relation between growth rate and driving force and on three types of growth mechanisms between smooth and rough interfaces. In Fig. 5, polyhedral crystals with internal skeleton structure are shown, in relation to their growth processes. They are the expected internal textures when a crystal grows at first on rough interface followed by smooth interface growth (route 1), and when it experiences smooth-rough-smooth growths (route 2). Internal textures of this sort seen in polyhedral single crystals have been observed among a wide variety of crystals. Typical examples are seen among snow crystals grown form the vapour, NaCl crystals grown from the aqueous solution, yttrium alminium garnet crystals grown from high temperature solution. Trapiche ruby is an additional example of such internal textures formed in nature.

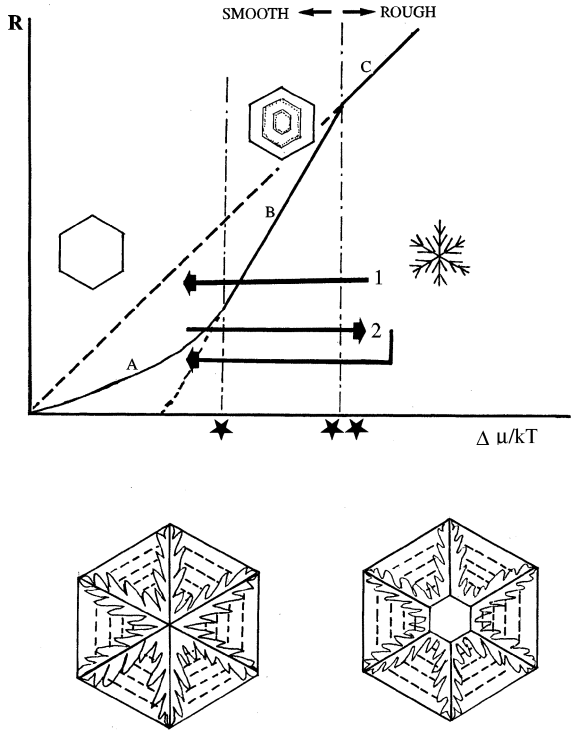

Fig. 5. Expected internal textures of a polyhedral crystal, when the crystal at first grew under higher driving force ($\Delta\mu/kT$) than **, followed by growth under lower driving force than ** (route 1), and when conditions changed from smooth, via rough, and again smooth interface growth (route 2). Curves A–C represent growth rate versus driving force relations for spiral growth (A), two-dimensional nucleation growth (B), and adhesive type growth (C). The critical points * and ** are the points where predominant growth mechanism changes. Modified from Ref. [5].

Irrespective of whether dendritic growth took place from the very beginning of corundum formation or whether it was preceded by the formation of transparent, single-phase ruby core, crystallographic orientations of dendritic arms and branches are the same. In the latter case, small ruby crystals were formed at first by layer-by-layer growth mechanism under small driving force condition. Then the driving force increased so that dendritic growth took place on the clear core. Dendritic growth takes place preferentially from the edges of a prismatic core crystal, where higher driving force is expected than that on the surface.

Change of driving force conditions during the formation of ruby crystals is reasonable, taking into consideration the conditional changes in contact metasomatic process. The trapiche rubies occur in contact metamorphosed marble, in a similar mode of occurrence as rubies in Mong Hsu, Myanmar [5]. Namely, they were formed when a magma intruded into carbonate strata. Depending on the contents and states of source clayed materials for corundum in carbonate rocks, and the positions from the magma intrusion, the driving force conditions are variable. It is anticipated that ordinary single ruby crystals, trapiche rubies without clear core, and those with clear core were formed depending on these conditions.

Trapiche emeralds show in many cases textures consisting of transparent better quality emerald core (tapered hexagonal prism), two-phase (albite-emerald) zone surrounding the core, two-phase arms and six growth sectors of transparent but poorer quality emerald [4]. Only rarely one may find trapiche emerald whose arms intersect at a small point. In trapiche ruby, the latter textures, i.e., without clear core, are more common. The difference between trapiche emerald and trapiche ruby is due to the difference between the geological setting of the two minerals. Trapiche emeralds occur in hydrothermally metasomatised country sedimental rocks adjacent to hydrothermal emerald veins.

3.2. Element partitioning

The observed differences in the contents and zoning of Cr and less distinctly those of Ti between growth sectors and arms and branches are good examples to demonstrate how element partitioning is governed.

When crystals of the same phase grow under different thermodynamic parameters, partition (distribution) coefficients of minor elements differ from each other. They are governed by thermodynamic parameters. When a crystal grows under nearly similar thermodynamic parameters and by the same growth mechanism, the effective distribution coefficients K_{eff}'s are governed by the kinetics. The K_{eff} for a smoother interface is higher than that for a rougher interface. The K_{eff} for a smooth interface

with higher normal growth rate (slower advancing rate of steps on the interface) is smaller than that with smaller normal growth rate (higher advancing rate of steps) [7]. In the same crystallographic orientation, chemical zoning appears parallel to the interface due to fluctuation of normal growth rate.

The observed distinct difference in Cr content and Cr zoning between the arms and growth sectors is due to the difference between rough and smooth interface growth. During the formation of dendritic growth on rough interface, partitioning of Cr was low and constant, close to the estimated Cr content in the original carbonate rocks. The growth was too rapid and the interface was too rough to accumulate impurity element at the interface. During the formation of growth sectors on smooth interface, partitioning of Cr increased almost eight times higher at first at the onset of layer growth, and decreased monotonously and increased again at the last stage. The origin of this variation or fluctuation is due to the growth rate changes and fluctuation on smooth $\{1\,1\,\bar{2}\,0\}$ and $\{0\,0\,0\,1\}$ interface. The Cr zoning appeared more distinctly in the slowest growth direction, parallel to $\{1\,1\,\bar{2}\,0\}$ faces, than in the higher growth direction, i.e., parallel to $\{0\,0\,0\,1\}$ faces, although both faces behaved as smooth interfaces.

3.3. Time required for growth and the origin of barrel-shaped habit

The main skeleton (and the present size of the crystal) of a trapiche ruby was constructed rapidly by dendritic growth, under a high driving force condition favourable for multi-phase precipitation of corundum, carbonates and un-identified K–Al–Fe–Ti silicates in fluid phase, i.e. dissolved carbonate mother rocks. Following the completion of the skeleton, i.e. of the present crystal size, or almost concurrently with that, but only at the dendrite roots, where a smaller driving force condition is assumed, more gentle growth took place on smooth interfaces to fill-in the interstices of dendrite arms and branches, eventually forming barrel-shaped corundum crystals. The origin of barrel-shaped habit of corundum bounded by high index hexagonal dipyramidal faces and $\{0\,0\,0\,1\}$ must be related to this growth process and associated element partitioning.

Following the argument in Ref. [4], the time required to complete the skeleton of trapiche ruby, and attaining the present size, must have been very short.

4. Conclusions

The unique textures seen in trapiche ruby, showing core, six arms, branches and six ruby growth sectors were formed by earlier dendritic growth on rough interfaces, under which eutectic type multiphase precipitation took place (opaque core, arms and branches), followed by later or concurrent filling-in process by layer-by-layer growth mechanism on smooth interfaces (growth sectors). Element partitioning was governed both by thermodynamic parameters (difference between growth sectors and core, arms and branches) and by kinetics (Cr zoning in growth sectors).

References

[1] K. Schmetzer, H.A. Hänni, H.-J. Bernhardt, D. Schwarz, Gem and Gemol. 32 (1996) 242.
[2] K. Schmetzer, H.A. Hänni, H.-J. Bernhardt, D. Schwarz, Goldschmiede Zeitung 95 (1997) 107.
[3] K. Schmetzer, B.L. Zhang, Y. Gao, H.-J. Bernhardt, H.A. Hänni, J. Gemmol. 26 (1998) 289.
[4] K. Nassau, K.A. Jackson, Amer. Mineral. 55 (1970) 416.
[5] A. Peretti, K. Schmetzer, H.-J. Bernhardt, F. Mouawad, Gem and Gemol. 31 (1995) 2.
[6] I. Sunagawa, in: I. Sunagawa (Ed.), Morphology of Crystals, Part B, Terra Science Publisher, Tokyo/Reidel, Dordrecht, p. 509.
[7] K.A. Jackson, 2nd Symposium Atomic-Scale Surface and Interface Dynamics, 26–27 February, 1998, Tokyo (invited talk).